Available online at www.sciencedirect.com
ScienceDirect
Ceramics International 34 (2008) 1941–1948
CERAMICS INTERNATIONAL
www.elsevier.com/locate/ceramint

Effects of A-site Ca and B-site Zr substitution on dielectric properties and microstructure in tin-doped $BaTiO_3$–$CaTiO_3$ composites

Man-Soon Yoon *, Soon-Chul Ur

Department of Material Science and Engineering/Research Center for Sustainable ECo-Devices and Materials (ReSEM), Chungju National University, Chungju, Chungbuk 380-702, Republic of Korea

Received 20 April 2007; received in revised form 12 May 2007; accepted 4 July 2007
Available online 10 August 2007

Abstract

In an effort to enhance dielectric properties and sinterability in a $BaTiO_3$–$CaTiO_3$ composite, substitution of Ca ion to Ba-site and Zr ion to Ti-site as well as tin doping were considered. Nominal forms of $(Ba_{1-x}Ca_x)(Ti_{0.96-y}Zr_ySn_{0.04})O_3$ $(0.15 \leq x \leq 0.20,\ 0.09 \leq y \leq 0.14)$ were synthesized by conventional solid-state processing technique, and their subsequent sinterability and dielectric properties were investigated. As Ca content was increased more than 15 mol%, the precipitation of second phase, whose main composition was $CaTiO_3$, started to form and the fraction of second phase was increased. Increase in Ca content appears to decrease the Curie temperature by the factor of 1.7°/mol% and to decrease the maximum dielectric constant by the factor of 200 $(mol\%)^{-1}$ possibly due to the effect of second phase having relatively lower dielectric constant. Increase in Zr content was also shown to decrease the Curie temperature by the factor of 10°/mol%, and to decrease the maximum dielectric constant by the factor of 217 $(mol\%)^{-1}$ presumably due to the increase of a diffuse phase transition (DPT). Sinterability and withstanding voltage characteristics were shown to improve by suppressing the abnormal grain growth due to the incorporation of second phases. An appropriate composition compatible with the Y5U (EIA standard) condenser which needs high breakdown voltage and dielectric constant is possible to be developed by controlling a DPT, in other words controlling the temperature stability, with incorporating Zr ion into the composite.

Keywords: C. Dielectric properties; $BaTiO_3$; $CaTiO_3$; DPT; Second phase

1. Introduction

Recently, the nonlinear nature of ferroelectrics has attracted much scientific and commercial attention because of its important applications in tunable microwave devices such as voltage-controlled oscillators and tunable filters and phase shifters [1–7]. Complying with recent technology trends in electronic devices of which circuits have been prone to integration with minimization, new classes of reliable dielectric materials, which need to show high performance in compact size but to be cheap, are under investigation. $BaTiO_3$ is most widely used ceramic dielectrics since it has relatively higher dielectric constants than those of current Al- and Ta-dielectrics, and its fabrication is relatively simple. However, the dielectric constant of single-phase $BaTiO_3$ at ambient temperature is only about 1500, though its temperature coefficient of capacitance (TCC) is notable. Most recent dielectric materials for high power condenser application show 7000–8000 of dielectric constant, and their TCC comply with the Y5U specification of electronic industry alliance (EIA) standard. Compositions for the condenser which meet Y5U specification are generally $BaTiO_3$-based solid solution in which substitution of Ca ion to Ba-site and Zr or Sn ion to Ti-site are applied to enhance dielectric constant at room temperature by shifting Curie temperature near to room temperature as well as to control TCC characteristic through the control of DPT behavior by addition of Sn or Zr. However, such solid solutions have frequently shown large fluctuations in room temperature dielectric constant due to abrupt grain growth resulting from sintering at high temperature, and have degraded the withstanding voltage characteristic due to relatively higher fraction of voids formed as a consequence of abnormal grain growth [8–11].

$CaTiO_3$ addition over the solubility limit into $BaTiO_3$ at sintering temperature was attempted to induce second-phase

* Corresponding author. Tel.: +82 43 841 5804; fax: +82 43 841 5805.
E-mail addresses: msyoon@cjnu.ac.kr (M.-S. Yoon), scur@cjnu.ac.kr (S.-C. Ur).

0272-8842/$34.00
doi:10.1016/j.ceramint.2007.07.010

formation, by which grain growth could be suppressed, so that fluctuations in room temperature dielectric constant could be diminished and the withstanding voltage characteristic could be enhanced in this study. In addition, a high-performance dielectric ceramic composite, which fulfills the temperature characteristic in Y5U specification, was attempted to develop by controlling DPT phenomena as a consequence of Zr ion addition.

2. Experimental procedure

Nominal compositions of perovskite $(Ba_{1-x}Ca_x)(-)(Ti_{0.96-y}Zr_ySn_{0.04})O_3$ $(0 \le x \le 0.2,\ 0.09 \le y \le 0.14)$ ceramics were fabricated by conventional solid-state processing technique. A commercial $BaTiO_3$ powders (BATIO, BT-01S) synthesized by an oxalate method, of which Ba/Ti mole ratio determined from XRF measurement appeared to be 0.995, were used as a main constituent. Additives used were $CaCO_3$ (Ube, 99%), TiO_2 (Tronox, 99.9%), ZrO_2 (Kojundo, EP grade) and SnO_2 (Kojundo, 99.9%). Bi_2O_3 (Kojundo, 99.9%) and SiO_2 (Kojundo, 99.9%) were used as sintering aids and $MnCO_3$ (Kojundo, 99.9%) was also used to reduce dielectric constant in the composite. Here, certain amounts of sintering aids were added into all the compositions in order to avoid their effects. Appropriately weighed powder mixtures were ball milled with ZrO_2 balls in an ethanol solution for 16 h. Dried powder mixtures were sieved under 100 mesh and then calcined at 1100 °C for 2 h followed by re-milling. In order to exclude the effect of milling effect on the subsequent sinterability, appropriate milling time was chosen based on the 90% cumulative particle size (D_{90}) to be 0.8 by observing the results from particle size analysis (Melvern Instrument Ltd. MICRO-P) during milling. After drying, the powders were sieved under 80 mesh and pressed uniaxially into discs (Ø15 mm) with a stress of 60 MPa followed by hydraulic pressing with a stress of 200 MPa. The compacts were sintered at 1320–1390 °C for 2 h with a heating rate of 5 °C/min. Sintered density was measured using a He pycnometer. Phase analyses for the sintered bodies were carried out using an X-ray diffractometer (XRD, Rigaku DMAX-3000) in the range of $2\theta = 20$–80° with a scan speed of 4°/min. After rough polishing up to #800 followed by thermal etching at 1220 °C for 20 min, microstructures were investigated using a scanning electron microscope (SEM; Hitachi S-2400), and chemical compositions were analyzed utilizing an energy dispersive spectroscopy (EDS; Kevex). In order to measure the electrical properties, Ga–In paste (Kojundo, 99.99%) was coated to form electrodes on both sides of the parallelepiped sample, then subsequently fired at 700 °C for 20 min. The dielectric properties and dielectric loss tangents were measured between the temperature ranges of −30 and 90 °C with 0.2° interval at 1 kHz using an impedance gain phase analyzer (HP-4194A) set combined with a temperature chamber (Delta-9023). After immersing samples in silicon oil bath, the withstanding voltages were measured under ac voltage using a withstanding voltage tester (Kikusui, TOS5101).

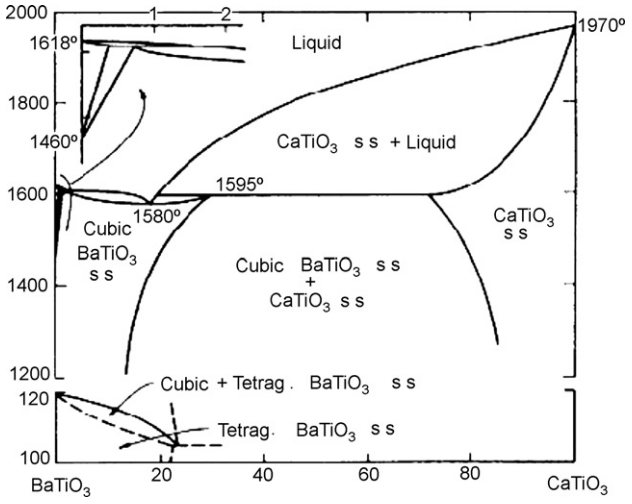

Fig. 1. $BaTiO_3$–$CaTiO_3$ phase diagram [12].

3. Results and discussion

3.1. Phase analysis

Fraction of $CaTiO_3$ experimented from 5 to 20 mol% indicates the coexistence of cubic $CaTiO_3$ with cubic $BaTiO_3$ at 1200 °C according to the equilibrium phase diagram [12] as presented in Fig. 1. Then, the mixed phase is supposed to become single-phase solid solution of cubic $BaTiO_3$ with increasing temperature above 1200 °C. Appropriate powder mixtures having CaO contents from 5 to 20 mol% with an interval of 1 mol% were compacted and sintered at 1320 °C for 2 h at which mixed phase region should exist. Phase analyses by XRD as a function of $CaTiO_3$ contents were presented in Fig. 2. Each XRD pattern represents typical $BaTiO_3$ without trace of second-phase formation. However, XRD result itself could not be a sole evidence for the presence of second phases, since low

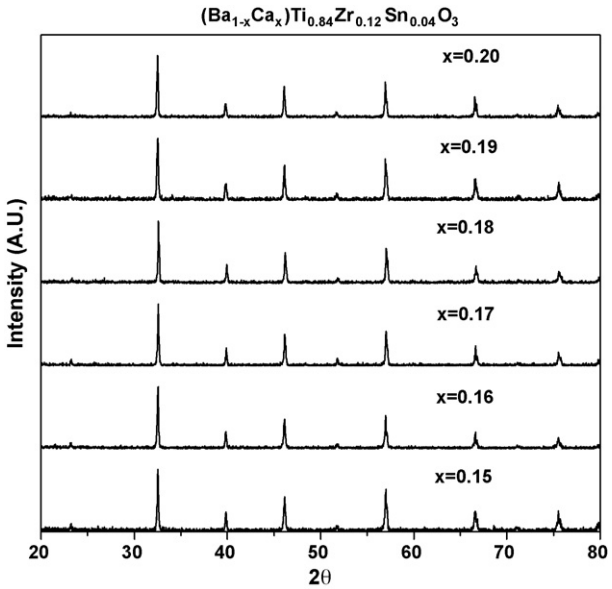

Fig. 2. X-ray diffraction patterns of sintered $(Ba_{1-x}Ca_x)(Ti_{0.84}Zr_{0.12}Sn_{0.04})O_3$ specimens containing various amounts of CaO.

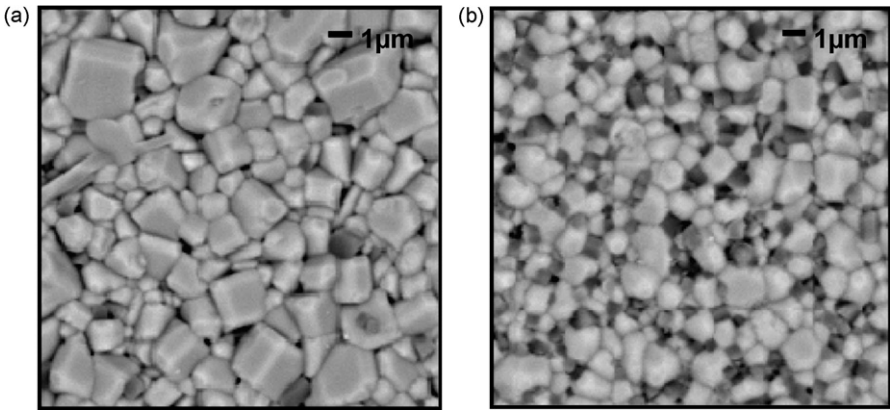

Fig. 3. SEM micrographs of polished and thermally etched surface of $(Ba_{1-x}Ca_x)(Ti_{0.84}Zr_{0.12}Sn_{0.04})O_3$ specimens sintered at 1320 °C for 2 h in air: (a) $x = 0.12$ and (b) $x = 0.20$.

fraction of second phases, typically less than 7 vol.%, could not be resolved by XRD. It is also difficult to resolve phases of they which were in the same perovskites structure [13]. In order to investigate the existence of second phases, microstructures of specimens containing 15 and 20 mol% CaO were examined as presented in Fig. 3(a) and (b). In the figures, second phases in black can be distinguished from matrix in white, and the fraction of second phases increased with increasing CaO contents. EDS analyses were carried out to examine the compositions of second phases in $(Ba_{0.8}Ca_{0.2})(Ti_{0.84}Zr_{0.12}Sn_{0.04})O_3$ as shown in Fig. 4. EDS spectra for matrix and second phase were presented in Fig. 4(a) and (b), respectively. As can be seen, Ba was revealed as a major element in matrix grains, suggesting that $BaTiO_3$ was a major component of matrix, while Ca contents were notable in second phases, suggesting that $CaTiO_3$ was a major component of second phases. Here, it is worth noting that second phases could not be detected in XRD analyses, since both $CaTiO_3$ and $BaTiO_3$ were of the same crystal structure.

3.2. Effect of additives on dielectric properties

3.2.1. Effect of CaO addition on dielectric properties

Effect of CaO addition in $(Ba_{1-x}Ca_x)(Ti_{0.84}Zr_{0.12}Sn_{0.04})O_3$ system on dielectric constant variations as a function of temperature was presented in Fig. 5. Each specimen examined was sintered at 1320 °C at which second phase might exist. As can be seen, Curie temperatures decreased with increasing CaO contents. Here, Curie temperature variation as a function of CaO contents was presented separately in Fig. 6. As CaO content was increased higher than 15 mol%, Curie temperature appeared to decrease by the factor of 1.7°/mol%. According to Herbert [14], such phenomenon was explained with the substitution of Ni^{2+} and/or Zn^{2+} ions for Ti^{4+} ions that leads to lattice shrinkage due to the formation of oxygen site vacancies for charge compensation, resulting in abrupt decrease in Curie temperature. On the other hand, it has been reported by Park et al. [15] and Yun et al. [16] that the lattice shrinkage arisen from the formation of oxygen site vacancies can be compensated in case of substitution of Ca^{2+} ions for Ti^{4+}, since the radius of Ca^{2+} ions is larger than that of Ti^{4+} ion, and then

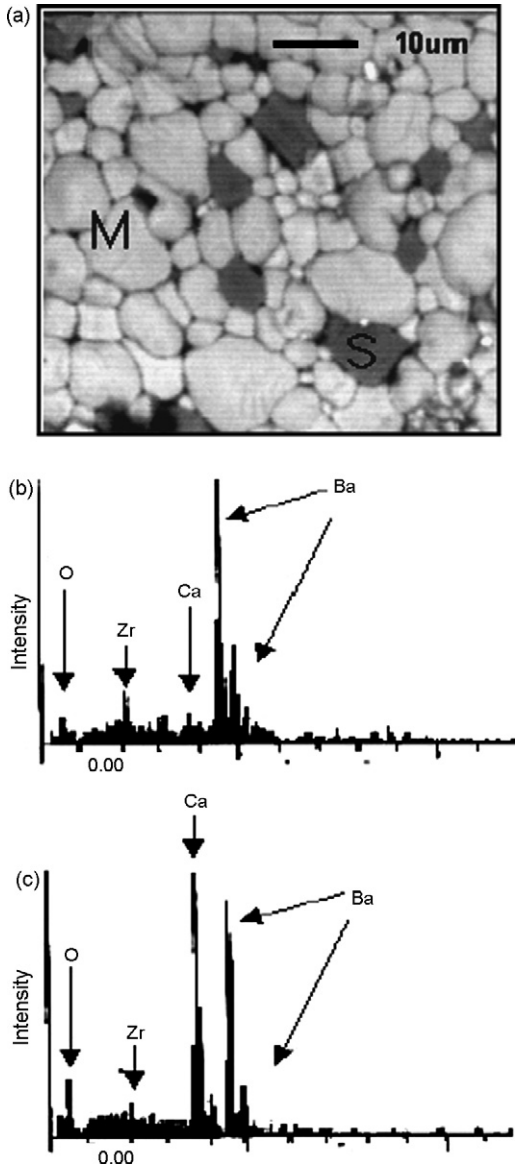

Fig. 4. (a) SEM micrograph showing second-phase grain in $(Ba_{0.8}Ca_{0.2})(Ti_{0.84}Zr_{0.12}Sn_{0.04})O_3$ specimen sintered at 1320 °C for 2 h in air and EDS spectra for (b) matrix grain and (c) second-phase grain.

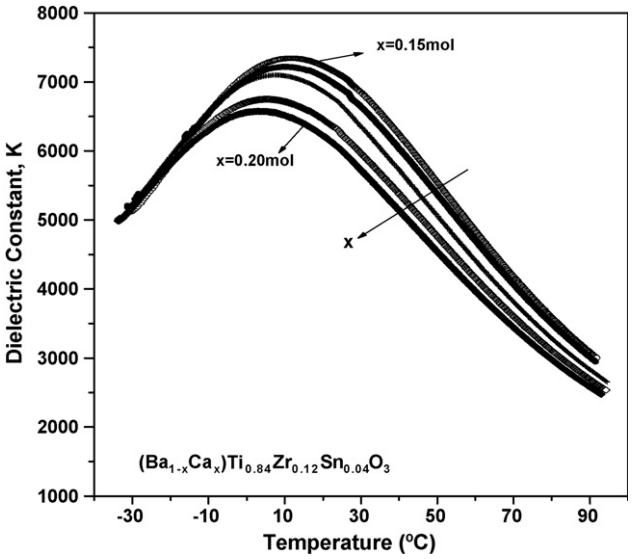

Fig. 5. Temperature dependence of dielectric constant (1 kHz) of $(Ba_{1-x}Ca_x)(-)(Ti_{0.84}Zr_{0.12}Sn_{0.04})O_3$ specimens containing various amounts of CaO.

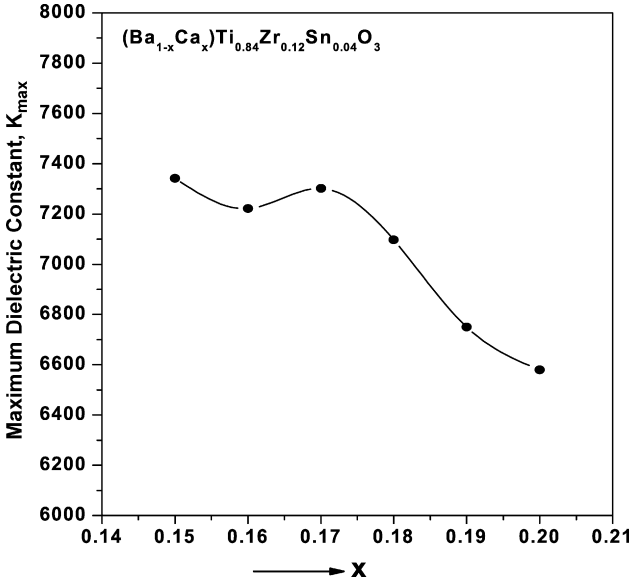

Fig. 7. Variation of maximum dielectric constants as a function of Ca contents (x) in $(Ba_{1-x}Ca_x)(Ti_{0.84}Zr_{0.12}Sn_{0.04})O_3$ specimen.

Curie temperature is decreased by the factor of 20°/mol% of Ca due to the compressive stresses exerting on adjacent lattices induced by lattice expansion. However, abrupt decrease in Curie temperature was not observed when Ca^{2+} was added higher than 15 mol% in this study and the fact was shown to be consistent with the result by Lin and Wu [17]. They reported that Curie temperature did not show to vary significantly when Ca^{2+} ions substituted for A-sites. Thus, Ca^{2+} ions added in this range here were believed to substitute with Ba-sites, and deduced to precipitate as second phases of $CaTiO_3$ in case of exceeding solubility limit. The variations of the maximum dielectric constants at Curie temperature as a function of CaO contents were also presented in Fig. 7. It can be seen that the maximum dielectric constant decreases by the factor of 200 $(mol\%)^{-1}$ with increasing CaO contents, possibly due to the effect of second phases of $CaTiO_3$ having relatively lower dielectric constant.

3.2.2. *Effect of ZrO_2 addition on dielectric properties*

Effect of ZrO_2 addition (9–14 mol%, with an interval of 1 mol%) in $(Ba_{0.85}Ca_{0.15})(Ti_{0.96-y}Zr_ySn_{0.04})O_3$ system on dielectric constant variation as a function of temperature was presented in Fig. 8. Each specimen examined was sintered at 1320 °C at which second phase might exist. Differently from the result of CaO addition, it can be seen that Curie temperature decreases abruptly and peak broadening becomes evident due to DPT with increasing ZrO_2 contents. In order to quantify this behavior, Curie temperature variation as a function of ZrO_2

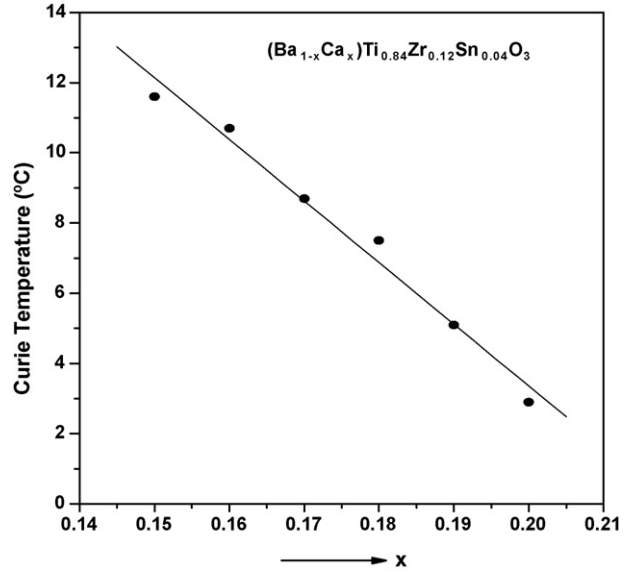

Fig. 6. Curie temperature variation as a function of Ca contents (x) in $(Ba_{1-x}Ca_x)(Ti_{0.84}Zr_{0.12}Sn_{0.04})O_3$ specimen.

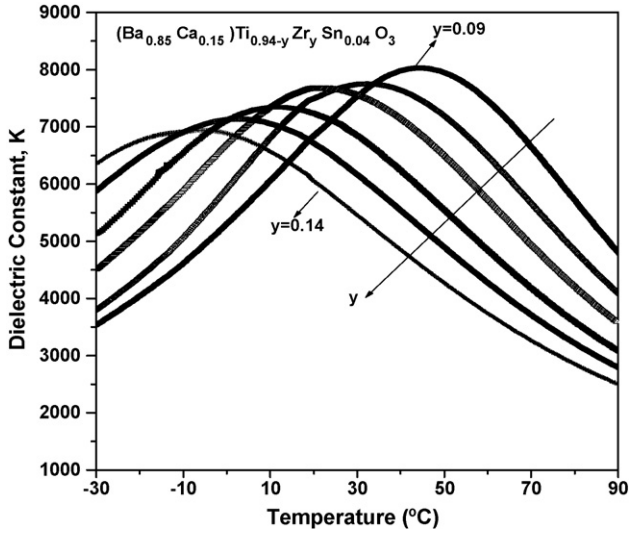

Fig. 8. Temperature dependence of dielectric constant (1 kHz) of $(Ba_{0.85}Ca_{0.15})(Ti_{0.96-y}Zr_ySn_{0.04})O_3$ specimens containing various amounts of CaO.

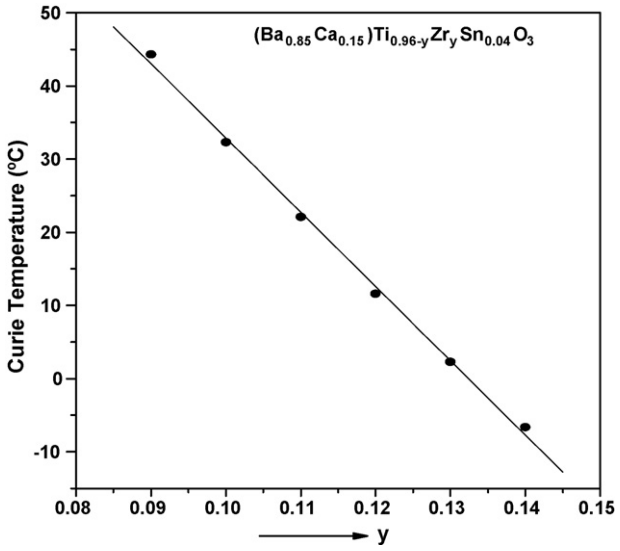

Fig. 9. Curie temperature variation as a function of Zr contents (y) in $(Ba_{0.85}Ca_{0.15})(Ti_{0.96-y}Zr_ySn_{0.04})O_3$ specimen.

contents was plotted as shown in Fig. 9. Curie temperature is decreased by the factor of 10°/mol% with increasing ZrO_2 contents. It can be noticed that Curie temperature was more significantly affected than that of CaO addition. Such an abrupt decrease in Curie temperature has, possibly, resulted from the substitution of larger Zr^{2+} ions with smaller Ti^{4+} ions that leads to the expansion in oxygen octahedron, inducing compressive stresses on adjacent lattices containing Ti^{4+} ions [17]. The variations of the maximum dielectric constants at Curie temperature as a function of ZrO_2 contents were also presented in Fig. 10. It can be seen that the maximum dielectric constant decreases the factor of 217 $(mol\%)^{-1}$ with increasing ZrO_2 contents, possibly due to protruding DPT phenomena in this case, since no second-phase formation occurred differently from CaO addition. According to Lin and Wu [17], substitution

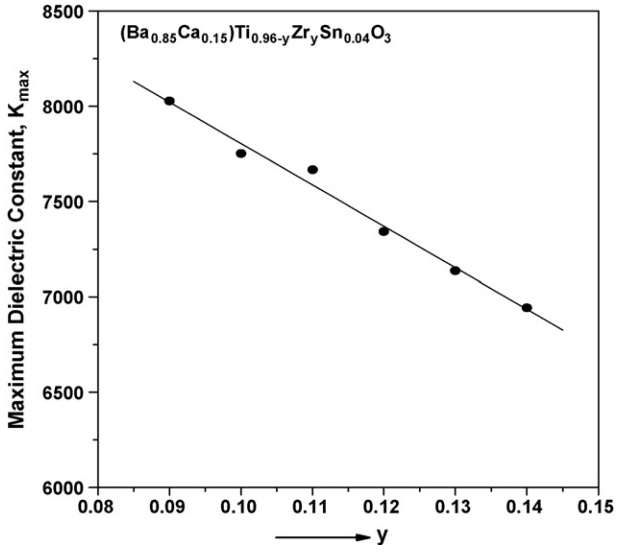

Fig. 10. Variation of maximum dielectric constants as a function of Zr contents (y) in $(Ba_{0.85}Ca_{0.15})(Ti_{0.96-y}Zr_ySn_{0.04})O_3$ specimen.

of Ca^{2+} ions for Ba^{2+} sites might induce the rearrangement of oxygen ions adjacent to Ca^{2+} ions to relocate more closely since the radius of Ba^{2+} ions is larger than that of Ca^{2+} ions, resulting in lattice strain in the direction of ⟨1 1 1⟩, but significant peak broadening by relaxor type DPT phenomena would not occur since the vibration in ⟨1 0 0⟩ direction of Ti^{4+} would not be affected as a consequence of a little effect of lattice strain on the direction of ⟨1 0 0⟩ in oxygen octahedron [17]. However, in case of the substitution of larger Zr^{2+} ions with smaller Ti^{4+} ions, space of ⟨1 0 0⟩ direction of Ti^{4+} could be reduced as a consequence of pushing oxygen ions in oxygen octahedron to ⟨1 0 0⟩ direction, and thus relaxor type DPT phenomena would be taken place as a result of the suppressed vibration of Ti^{4+} ions. Hence the decrease in dielectric constant at Curie temperature could be due to the decrease in spontaneous polarization of Ti^{4+} ions.

3.3. Effect of sintering temperature on microstructures

In order to observe microstructure variations during syntheses, compositions of $(Ba_{0.85}CaO_{0.15})(Ti_{0.84}Zr_{0.12}Sn_{0.04})O_3$ and $(Ba_{0.82}CaO_{0.18})(Ti_{0.84}Zr_{0.12}Sn_{0.04})O_3$ sintered at 1320–1380 °C for 2 h were examined as presented in Fig. 11. In case of 15 mol% of CaO addition, second phases with a size of 1 μm precipitated during sintering at 1320 °C throughout the matrix with a grain size of 2–3 μm can be seen in Fig. 11(a)–(c). In case of sintering at 1340 °C, apparent fraction of second phases was decreased, and some grains in matrix grew abnormally, resulting in bimodal grain distribution with sizes of 10 and 1 μm. In case of sintering at 1380 °C, second phases were hardly seen, and the fraction of grains grown abnormally was increased with consuming smaller sized grains until impinging each other, resulting in a normal distribution as in normal grain growth behavior. As can be expected from the equilibrium phase diagram [13], at the temperature range, where $BaTiO_3$ and $CaTiO_3$ coexist, homogeneous fine microstructure appears. It seems that the existence of $CaTiO_3$ second phase increases the diffusion path of material between the grains, and consequently prohibits grain growth [18,19], but the fraction of second phases decreases as sintering temperature increases due to the increase in solubility of $CaTiO_3$ in $BaTiO_3$. Here, it is worthy noting that abnormal grain growth can be induced at selective area where second phases are diminished, as shown in Fig. 11(b). These results can be designated pinning effect of second phase.

On the other hand, in case of 18 mol% of CaO addition, the fraction of $CaTiO_3$ second phases revealed to increase and the grain sizes of second phase and matrix were apparently similar to each other with a size of 1 μm in the final microstructure after sintering at 1320 °C, as shown in Fig. 11(d)–(f), differently from those in 15 mol% of CaO addition. As sintering temperature increases up to 1380 °C, abnormal grain growth behavior in matrix appears to be suppressed somewhat possibly due to the decrease in the pinning effect of second phases which grow concurrently with matrix grains [13]. The fact that abnormal grain growth took place at 1340 °C in case of 15 mol% of CaO addition while normal grain growth behavior was shown in case of 18 mol% of CaO addition can be explained as a consequence

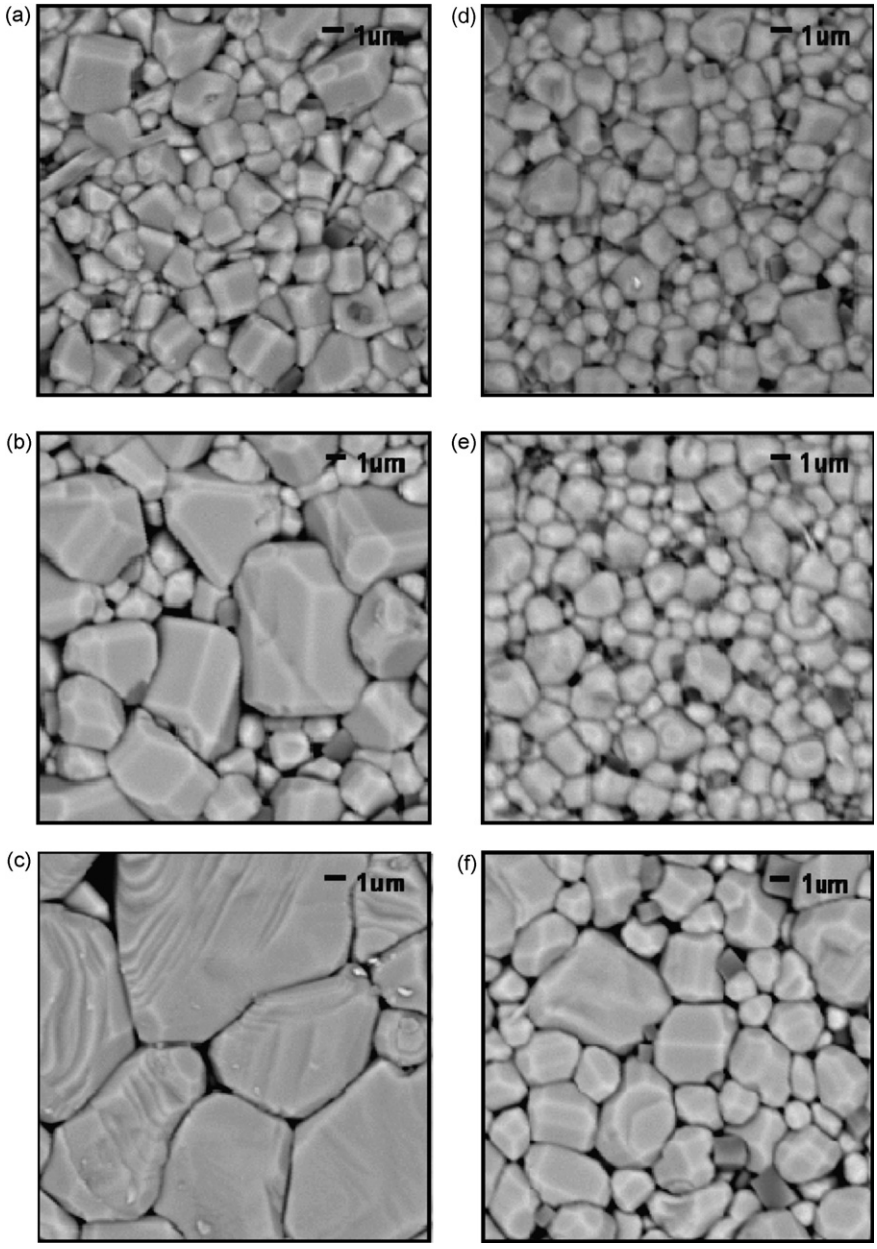

Fig. 11. SEM micrographs of polished and thermally etched surface of $(Ba_{1-x}Ca_x)(Ti_{0.84}Zr_{0.12}Sn_{0.04})O_3$ specimens sintered at various temperature for 2 h in air: (a)–(c) for $x = 0.12$, (d)–(f) for $x = 0.18$, (a) and (d) sintered at 1320 °C, (b) and (e) sintered at 1340 °C, and (c) and (f) sintered at 1380 °C.

of the increase in second-phase fraction with increasing CaO contents in case of 18 mol% of CaO addition. The pinning effect would then be distributed all over the matrix, and second phases might be stable up to 1380 °C.

From the discussions above, it is considered that stability in microstructure can be attributed to the maximization of the second-phase fraction by increasing CaO contents, depending on desired dielectric constants and TCC characteristics. As a consequence, stabilization of microstructures during sintering might be expected to contribute to the stability of the dielectric constant at room temperature and density for high power condenser applications. In order to verify this hypothesis, dielectric constants at room temperature for the compositions of $(Ba_{0.85}CaO_{0.15})(Ti_{0.84}Zr_{0.12}Sn_{0.04})O_3$ and $(Ba_{0.82}CaO_{0.18})(Ti_{0.84}Zr_{0.12}Sn_{0.04})O_3$ as a function of sintering temperature were plotted as shown in Fig. 12. It is observed that the dielectric constants at room temperature rapidly increase between 1340 and 1370 °C in case of 15 mol% of CaO addition compared with 18 mol% of CaO addition. It is also noticed that dielectric constants at room temperature show a plateau of 8000 in case of 18 mol% of CaO addition.

3.4. Effect of sintering stability on the withstanding voltage characteristic and density

Sintered densities of $(Ba_{0.85}CaO_{0.15})(Ti_{0.84}Zr_{0.12}Sn_{0.04})O_3$ and $(Ba_{0.82}CaO_{0.18})(Ti_{0.84}Zr_{0.12}Sn_{0.04})O_3$ as a function of sintering temperature were presented in Fig. 13. Densities

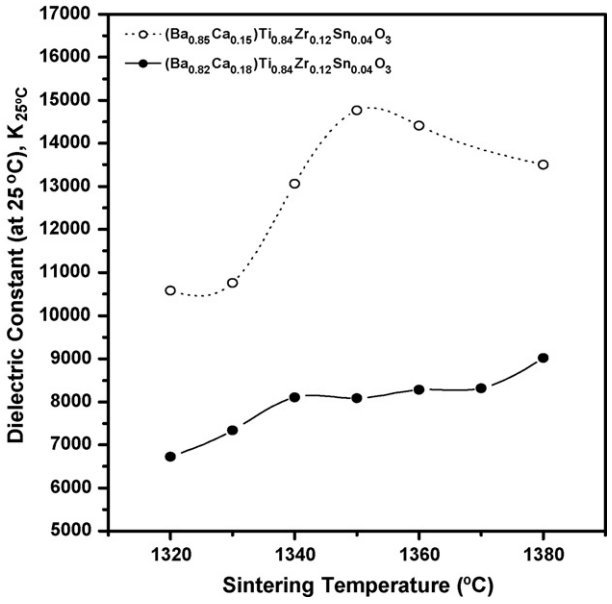

Fig. 12. Variation of dielectric constant at room temperature and 1 kHz as a function of sintering temperature for $(Ba_{0.85}Ca_{0.15})(Ti_{0.84}Zr_{0.12}Sn_{0.04})O_3$ and $(Ba_{0.82}Ca_{0.18})(Ti_{0.84}Zr_{0.12}Sn_{0.04})O_3$ compositions.

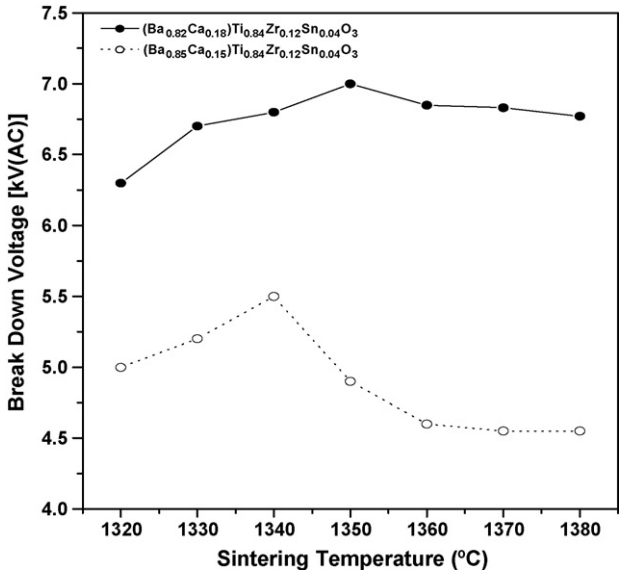

Fig. 14. Variation of withstanding voltage as a function of sintering temperature for $(Ba_{0.85}Ca_{0.15})(Ti_{0.84}Zr_{0.12}Sn_{0.04})O_3$ and $(Ba_{0.82}Ca_{0.18})(Ti_{0.84}Zr_{0.12}Sn_{0.04})O_3$ compositions.

are shown to remain nearly constant with increasing second-phase fraction in $(Ba_{0.82}CaO_{0.18})(Ti_{0.84}Zr_{0.12}Sn_{0.04})$, while the densities of $(Ba_{0.85}CaO_{0.15})(Ti_{0.84}Zr_{0.12}Sn_{0.04})O_3$ showed a maximum at 1340 °C at which second phases began to diminish, and then densities were decreased gradually afterwards. Such behavior is believed to attribute to the increase in voids during abnormal grain growth. The withstanding voltage characteristic under ac electric field revealed to be very similar to density variations as shown in Fig. 14. It is also noticed that the withstanding voltage increases up to 7 kV according to the stabilization of second phases with increasing temperature.

3.5. TCC characteristics in $BaTiO_3$–$CaTiO_3$ composites

In order to assess TCC characteristic in a composite of $(Ba_{0.82}CaO_{0.18})(Ti_{0.84}Zr_{0.12}Sn_{0.04})O_3$, which should show reliable sintering stability and high withstanding voltage, TCC (%) for samples sintered at 1340 °C for 2 h was measured and calculated using Eq. (1) in the temperature range of −30 to 85 °C, as presented in Fig. 15:

$$\mathrm{TCC}\,(\%) = \frac{C_T - C_{25\,^\circ\mathrm{C}}}{C_{25\,^\circ\mathrm{C}}} \times 100 \quad (1)$$

TCC variation obtained is +6 and −53%, which appears to be consistent with the EIA specification of +22 and −56%.

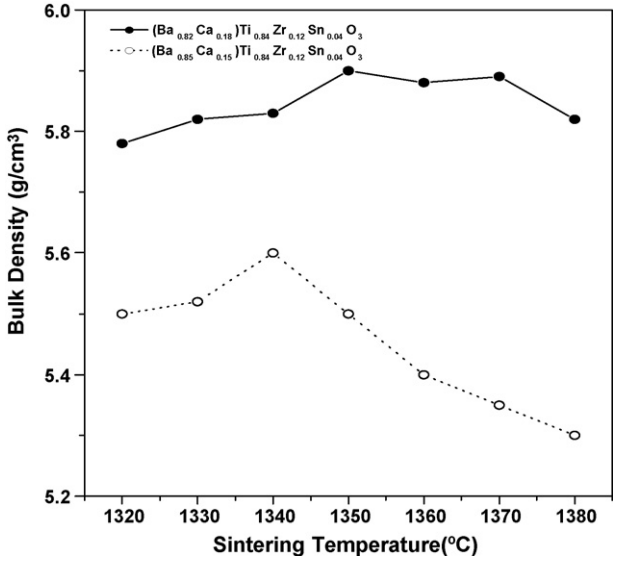

Fig. 13. Variation of sintered density as a function of sintering temperature for $(Ba_{0.85}Ca_{0.15})(Ti_{0.84}Zr_{0.12}Sn_{0.04})O_3$ and $(Ba_{0.82}Ca_{0.18})(Ti_{0.84}Zr_{0.12}Sn_{0.04})O_3$ compositions.

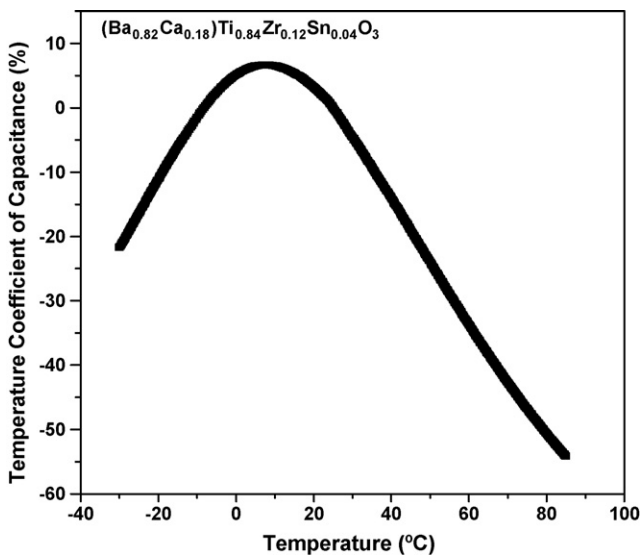

Fig. 15. Variation of temperature coefficient of capacitance as a function of temperature for $(Ba_{0.82}Ca_{0.18})(Ti_{0.84}Zr_{0.12}Sn_{0.04})O_3$ specimen sintered at 1340 °C.

4. Conclusion

In an effort to enhance dielectric properties and sinterability in a $BaTiO_3$–$CaTiO_3$ composite, substitution of Ca ion to Ba-site and Zr ion to Ti-site as well as tin doping were considered. Nominal forms of $(Ba_{1-x}Ca_x)(Ti_{0.96-y}Zr_ySn_{0.04})O_3$ ($0.15 \leq x \leq 0.20$, $0.09 \leq y \leq 0.14$) were synthesized by conventional solid-state processing technique, and their subsequent sinterability and dielectric properties were investigated as follows:

(1) As Ca content was increased more than 15 mol%, the precipitation of second phase, whose main composition was $CaTiO_3$, started to form and the fraction of second phase was increased.
(2) Increase in Ca content appears to decrease the Curie temperature by the factor of 1.7°/mol% and to decrease the maximum dielectric constant by the factor of 200 $(mol\%)^{-1}$ possibly due to the effect of second phase having relatively lower dielectric constant.
(3) Increase in Zr content appears to decrease the Curie temperature by the factor of 10°/mol% as well as to decrease the maximum dielectric constant by the factor of 217 $(mol\%)^{-1}$ due to introducing compressive strains into the spontaneous polarization $\langle 1\,0\,0 \rangle$ direction of Ti^{4+} ions as a consequence of the increase of a diffuse phase transition.
(4) In case of 15 mol% of CaO addition, apparent fraction of second phases was decreased, and some grains in matrix grew abnormally during sintering at 1340 °C, while fraction of second phases remains constant and abnormal grain growth behavior was shown to suppress in case of 18 mol% of CaO addition at the sintering temperature range of 1340–1370 °C. The dielectric constants at room temperature show a plateau of 8000 between 1340 and 1370 °C in case of 18 mol% of CaO addition.
(5) Sinterability and withstanding voltage characteristics were shown to improve due to the incorporation of second phases. Existence of second phase was also shown to stabilize the dielectric constant at room temperature.
(6) An appropriate composition of $(Ba_{0.82}Ca_{0.18})(Ti_{0.96-y}Zr_ySn_{0.04})O_3$ composite compatible with the Y5U (EIA standard) condenser which needs high breakdown voltage and dielectric constant is possible to be developed by controlling a DPT. With incorporating 12 mol% of Zr ion into the composite, it was obtained that dielectric constant at room temperature is 8000, and TCC variation is +6 to −53% in the temperature range of −30 to 85 °C, which satisfy the EIA specification.

Acknowledgements

This research was supported by the Program for the Training of Graduate Students in Regional Strategic Industries and Regional Innovation Center (RIC) Program which was conducted by the Ministry of Commerce, Industry and Energy of the Korean Government.

References

[1] X.X. Xi, H.C. Li, W.D. Si, I.A. Akimov, J.R. Fox, A.M. Clark, J.H. Hao, Oxide thin films for tunable microwave devices, J. Electroceram. 4 (2000) 393–405.
[2] R.E. Treece, J.B. Thompson, C.H. Mueller, T. Rivkin, M.W. Cromar, Optimization of $SrTiO_3$ for applications in tunable resonant circuits, IEEE Trans. Appl. Supercond. 7 (1997) 2363–2366.
[3] H.C. Li, W.D. Si, A.D. West, X.X. Xi, Near single crystal-level dielectric loss and nonlinearity in pulsed laser deposited $SrTiO_3$ thin films, Appl. Phys. Lett. 73 (1998) 190–192.
[4] A.B. Kozyrev, T.B. Samoilova, A.A. Golovkov, E.K. Hollmann, D.A. Kalinikos, V.E. Loginov, A.M. Prudan, O.I. Soldatenkov, D. Galt, C.H. Mueller, T.V. Rivkin, G.A. Koepf, Nonlinear behavior of thin film $SrTiO_3$ capacitors at microwave frequencies, J. Appl. Phys. 84 (1998) 3326–3332.
[5] C.L. Chen, H.H. Feng, Z. Zhang, A. Brazdeikis, Z.J. Huang, W.K. Chu, C.W. Chu, F.A. Miranda, F.W. Van Keuls, R.R. Romanofsky, Epitaxial ferroelectric $Ba_{0.5}Sr_{0.5}TiO_3$ thin films for room-temperature tunable element applications, Appl. Phys. Lett. 75 (1999) 412–414.
[6] A. Outzourhit, J.U. Trefny, T. Kito, B. Yarar, Tunability of the dielectric constant of $Ba_{0.1}Sr_{0.9}TiO_3$ ceramics in the paraelectric state, J. Mater. Res. 10 (1995) 1411–1415.
[7] W.T. Chang, L. Sengupta, MgO-mixed $Ba_{0.6}Sr_{0.4}TiO_3$ bulk ceramics and thin films for tunable microwave applications, J. Appl. Phys. 92 (2002) 3941–3946.
[8] D. Hennings, Barium titanate based ceramic materials for dielectric use, Int. J. High Tech. Ceram. 3 (1987) 91–111.
[9] G.H. Jonker, A.L. Stuijts, Controlling the properties of electroceramic materials through there microstructure, Philips Tech. Rev. 32 (1971) 72–95.
[10] P. Chantikul, S.J. Bennison, B.R. Lawn, Role of grain size in the strength and R-curve properties of alumina, J. Am. Ceram. Soc. 73 (1990) 2419–2427.
[11] M. Hillert, On the theory of normal and abnormal grain growth, Acta Metall. 13 (1965) 227–238.
[12] R.C. Devries, R. Roy, Phase equilibria in the system $BaTiO_3$–$CaTiO_3$, J. Am. Ceram. Soc. 38 (1995) 142–146.
[13] X.M. Chen, T. Wang, J. Li, Dielectric characteristics and their field dependence of (Ba, Ca)TiO_3 ceramics, Mater. Sci. Eng. B 113 (2004) 117–120.
[14] J.M. Herbert, Ceramic Dielectric and Capacitor, Gordon and Breach Science Publishers, New York, 1985, pp. 117–120.
[15] J.S. Park, T.S. Oh, Y.H. Kim, Effects of A-site Sr and B-site Ca substitution on the dielectric properties of $BaTiO_3$ ceramics, J. Kor. Ceram. Soc. 38 (1991) 689–695.
[16] S. Yun, X. Wang, Dielectric properties of bismuth doped $Ba_{1-x}Ca_xTiO_3$ ceramics, Mater. Lett. 60 (2006) 2211–2213.
[17] J.N. Lin, T.B. Wu, Effect of isovalent substitutions on the lattice softening and transition character of $BaTiO_3$ solid solutions, J. Appl. Phys. 68 (1990) 985–993.
[18] Y. Matsuo, H. Sasaki, Exaggerated grain growth in liquid-phase sintering of $BaTiO_3$, J. Am. Ceram. Soc. 54 (1971) 471–478.
[19] D.F.K. Hennings, R. Janssen, P.J.L. Reynen, Control of liquid-phase-enhanced discontinuous grain growth in barium titanate, J. Am. Ceram. Soc. 70 (1987) 23–27.